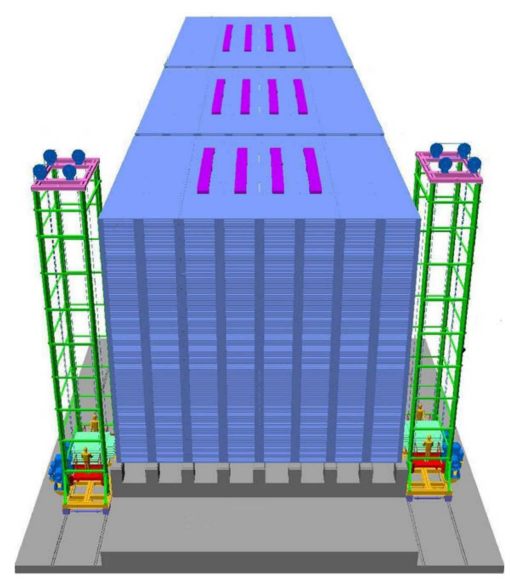
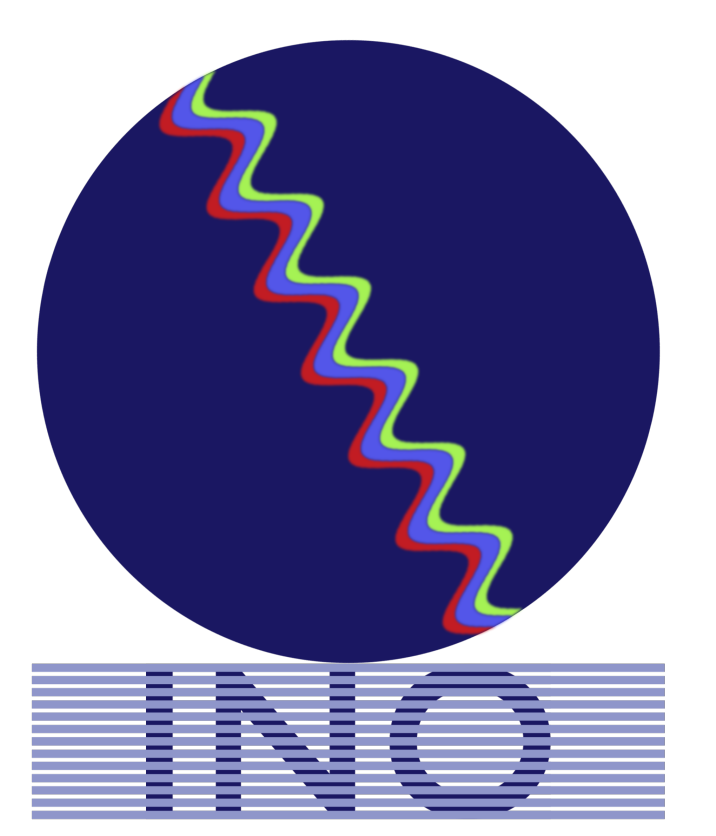


CHARGE RATIO OF COSMIC MUON SPECTRUM AT MADURAI, INDIA

J. M. John^{1,2}, Raj Shah^{1,2}, G. Majumder²

¹ Homi Bhabha National Institute, Mumbai-400094,

² Tata Institute of Fundamental Research, Mumbai-400005,
jimmjohn007@gmail.com

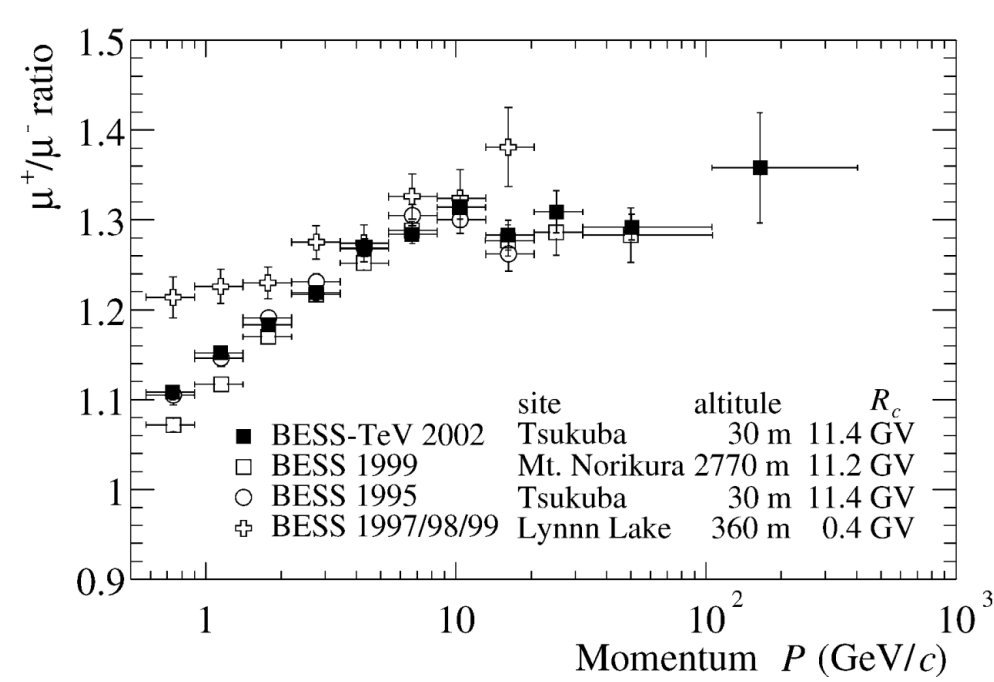


INTRODUCTION

The mini-ICAL is a small prototype of the 50 kton iron calorimeter detector (ICAL) is commissioned in IICHEP transit campus. The prototype is made of iron of size 4 m×4 m, weighing approximately 85 tons. It has been taking cosmic ray muon data since August, 2018 within the IICHEP, Madurai (9°56'N, 78°00'E) until 2023.

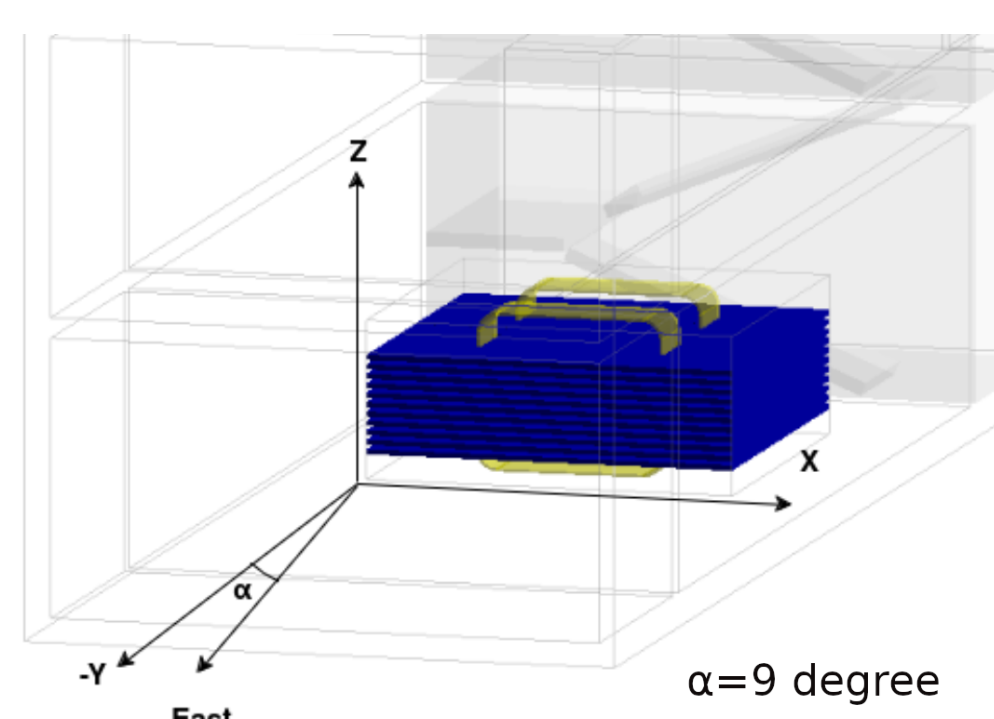
LITERATURE SURVEY

There were few measurements in cosmic rays in this energy range. One was with the Balloon-borne Experiment with a Superconducting Spectrometer (BESS) [1]. The μ^+/μ^- charge ratio can vary between 1.1 to 1.2 in this energy range for a rigidity cutoff of ~ 11 GeV at Tsukuba location [2]. The vertical geomagnetic rigidity cutoff for Madurai is ~ 17.4 GeV.



BESS spectrometer focuses on near vertical cosmic muons upto zenith angle $\sim 17^\circ$, whereas this measurement is extended upto 50° .

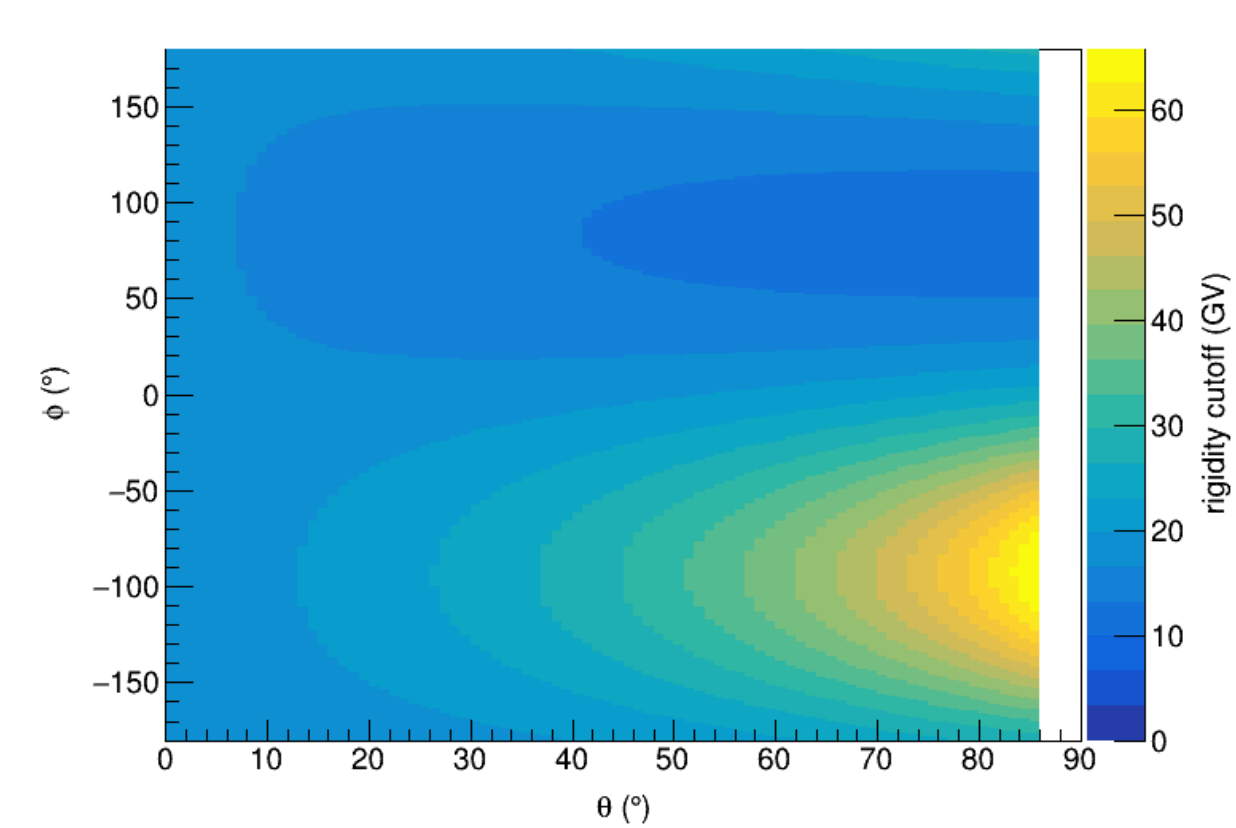
EXPERIMENTAL SETUP



- 11 layers of iron plates with 10 RPCs interspersed between them.
- Large area RPCs (175 cm × 185 cm).
- The detector is magnetized by passing about 900 amp direct current.
- Each RPC contain two pickup panels places orthogonally on both sides of the RPC to precisely locate the traversing particle's position.

CORSIKA SIMULATION

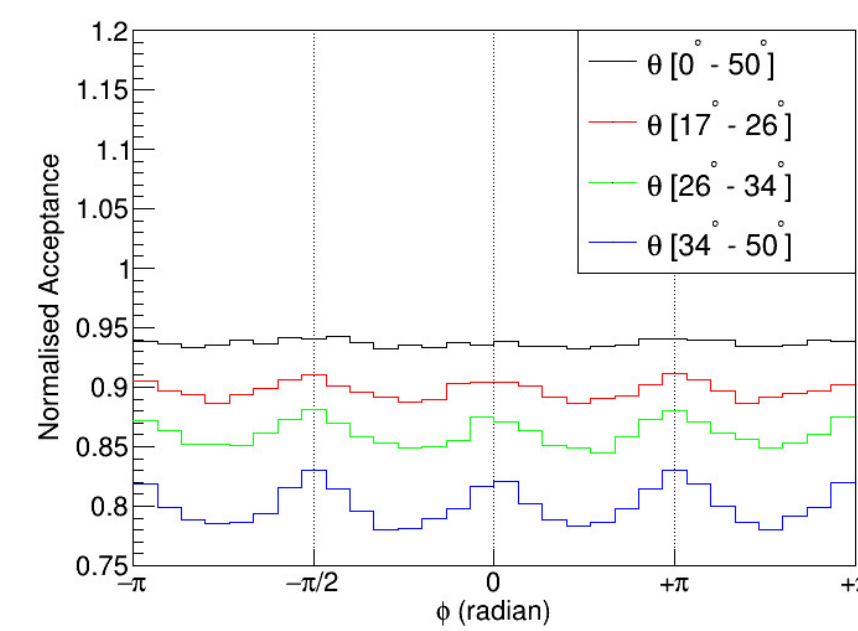
Low energy - FLUKA & GHEISHA
High energy - SIBYLL, QGSJET 01C, QGSJETII 04, VENUS



REFERENCES

[1] T. Sanuki *et al.* *Precise measurement of cosmic-ray proton and helium spectra with the BESS spectrometer.* The Astrophysical Journal, 545(2):1135 dec 2000.
[2] M Motoki *et al.* *Precise measurements of atmospheric muon fluxes with the BESS spectrometer.* Astropart. Phys., 19:113–126, 2003
[3] S Schmitt. *Tunfold, an algorithm for correcting migration effects in high energy physics.* Journal of Instrumentation, 7(10):T10003, oct 2012
[4] S Schmitt. *Data unfolding methods in high energy physics.* EPJ Web Conf., 137:11008, 2017.

ACCEPTANCE



The Acceptance is just the ratio of events which pass the trigger selection criteria to the total events generated in the particular bin.

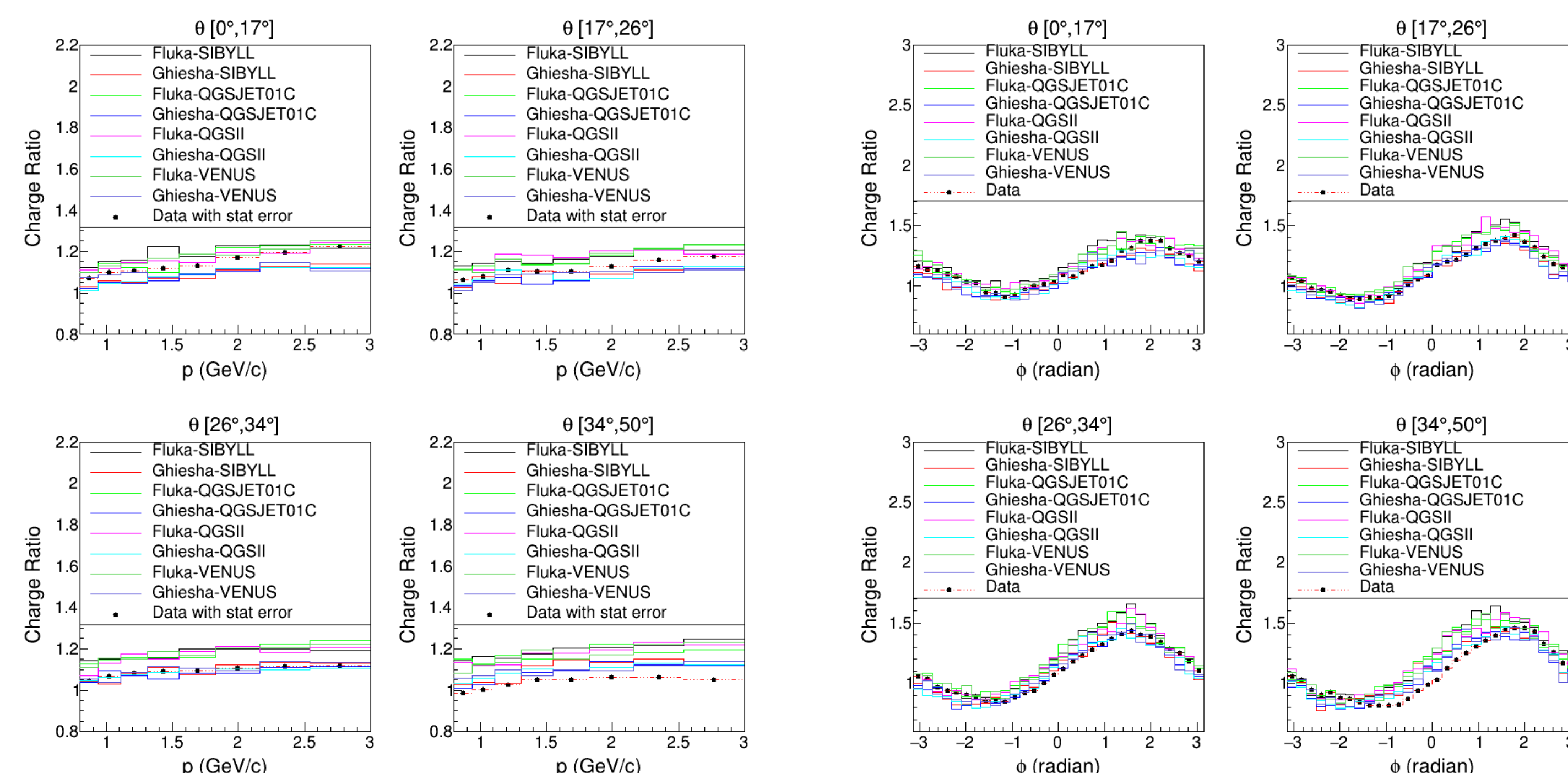
DATA ANALYSIS

- 1 Once the trigger (hit in top four layers) is formed, the hit information is collected till $\sim 21 \mu s$ after the trigger time.
- 2 Initial offset correction for both time and position
- 3 Use only hits within $\Delta t \leq \pm 5$ ns of the expected hit in the top layers is used for fitting.
- 4 In a specific Z plane, all potential combinations of X and Y strips within a ± 5 ns window are combined to generate 2D-hits position.
- 5 The event selection process employs a track finder algorithm.
- 6 The reconstruction of events employs a Kalman filter algorithm
- 7 The state vector is characterized by $(x, y, dx/dz, dy/dz, q/p)$.
- 8 Measurement errors arise due to strip width, inefficiency and other factors, with the extrapolation error defined by a propagator matrix.
- 9 An iterative procedure of calculating the kalman gain and estimating state vector at each layer is employed.
- 10 Finally, the q/p value, along with azimuthal and zenith angles, is determined on the topmost layer of RPC with a measured point.
- 11 Quality cuts are applied with p-value and number of layer in fit.

The fractions of events retained after the application of each cuts/selection.

	Data	Simulation
Total Events	$N = 70 \times 10^6$	24×10^6
criteria	Fraction Retained	
No criteria	1.0	1.0
trigg events	1.0	0.78
reco/trigg	0.86	0.88
sel/trigg	0.76	0.78

CHARGE RATIO



SUMMARY

The charge ratio is defined by $R_\mu = \frac{N_{\mu^+}}{N_{\mu^-}}$. The charge ratio with respect to momentum shows a systematic reduction with larger zenith angles. The study by [2] indicates that with a higher rigidity cutoff, the momentum charge ratio decreases. At an 11 GV rigidity cutoff, within the same momentum range, the ratio falls between 1.1 and 1.2 in their study. However, [2] primarily observed smaller zenith angles, aligning with our findings in the range of 0° to 17° . Yet, at larger zenith angles, the ratio appears to decrease, an observation not reported in the literature for this energy range and zenith angle.

UNFOLDING

- The impacts of detector effects and statistical fluctuations can result in events being reconstructed in incorrect momentum/ ϕ bins or potentially lost.
- Both the bin migration and the inefficiency can be mathematically expressed in the following way.

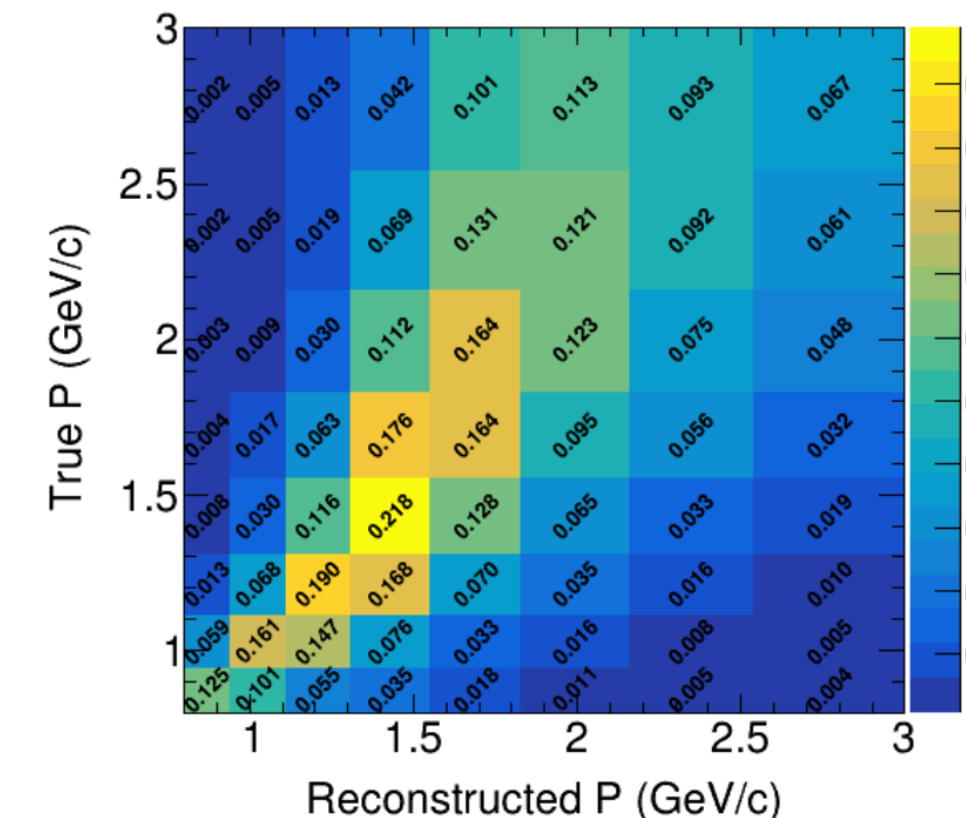
$$\sum_{j=1}^m \mathbf{A}_{ij} \mathbf{x}_j + \mathbf{b}_i = \mathbf{y}_i \quad (1)$$

where \mathbf{x} is the generator level vector of dimension \mathbf{m} , \mathbf{y} is the detector level vector of dimension \mathbf{n} , and \mathbf{A} is the response matrix with elements \mathbf{A}_{ij} specify the probability to find an event generated in bin \mathbf{j} to be measured in bin \mathbf{i} .

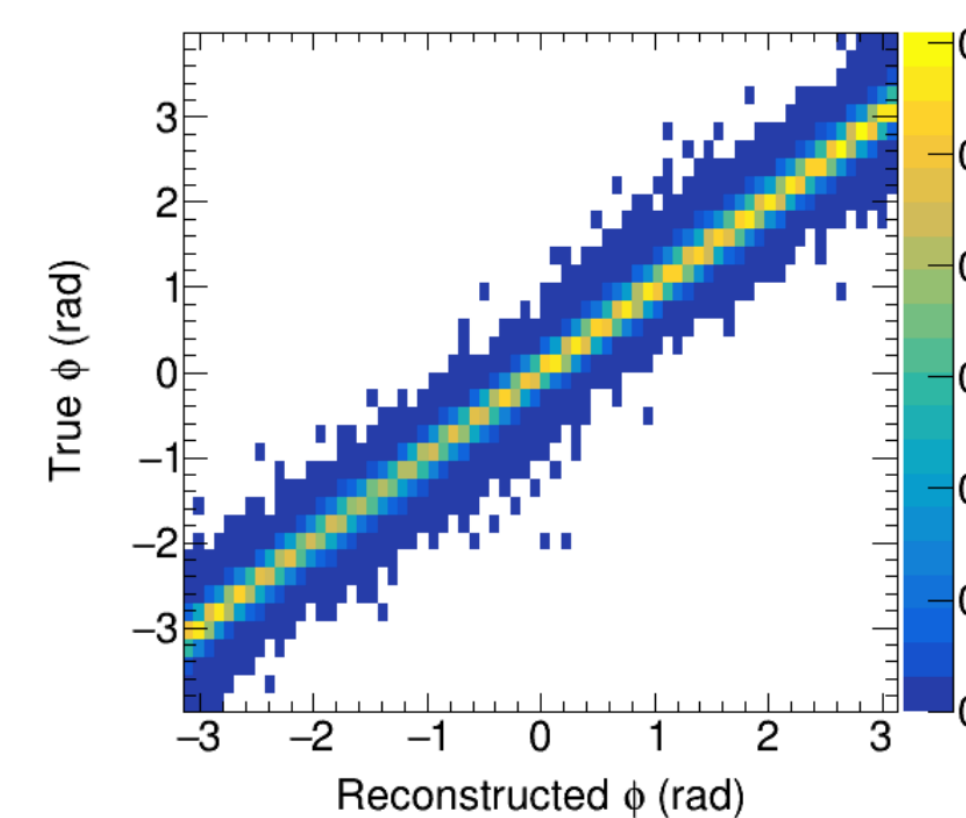
THE RESPONSE MATRIX

The response matrix and the background (b) is estimated using the monte carlo simulation.

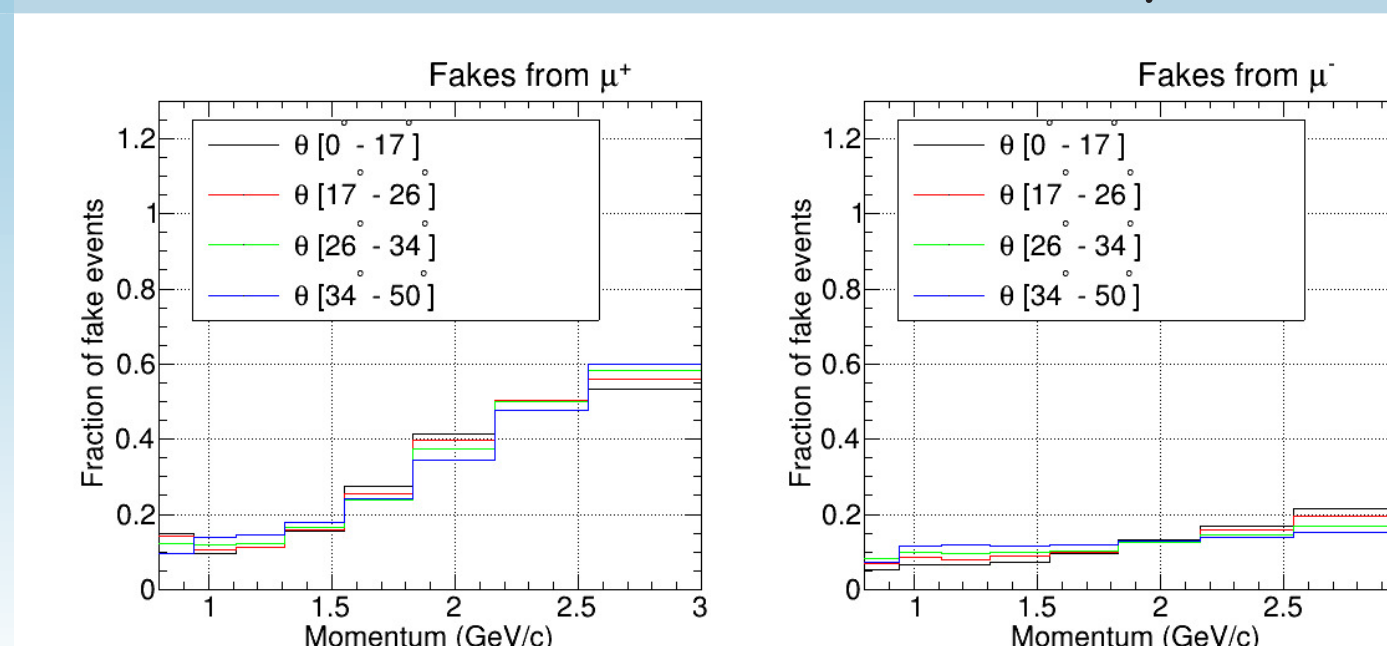
Momentum Response Matrix



Azimuth Response Matrix



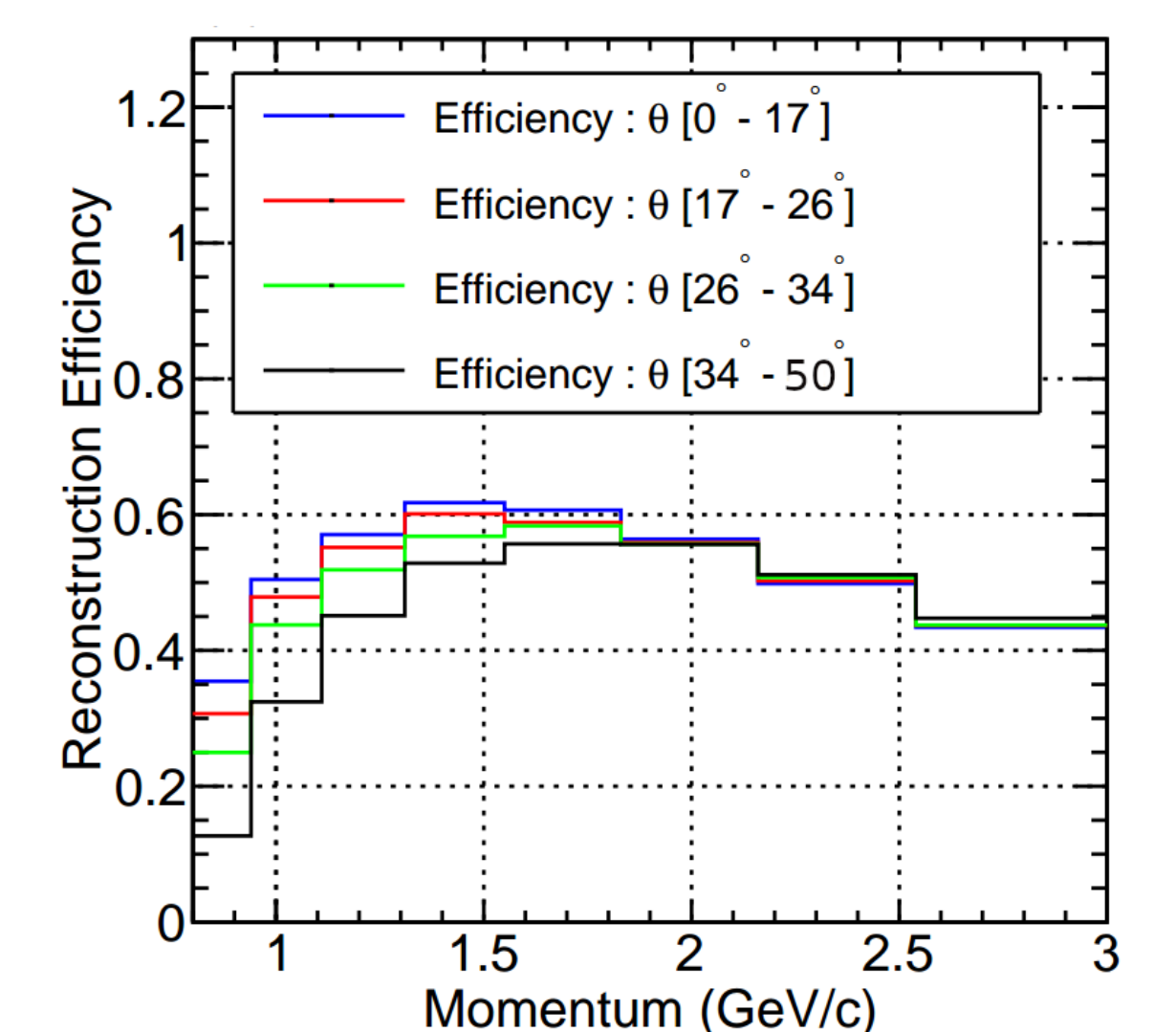
THE FAKE RATE FOR μ^+



MINI-ICAL STACK



RECO EFFICIENCY



Both the unfolded spectra are corrected for both efficiency and the fake rates.

REGULARIZATION

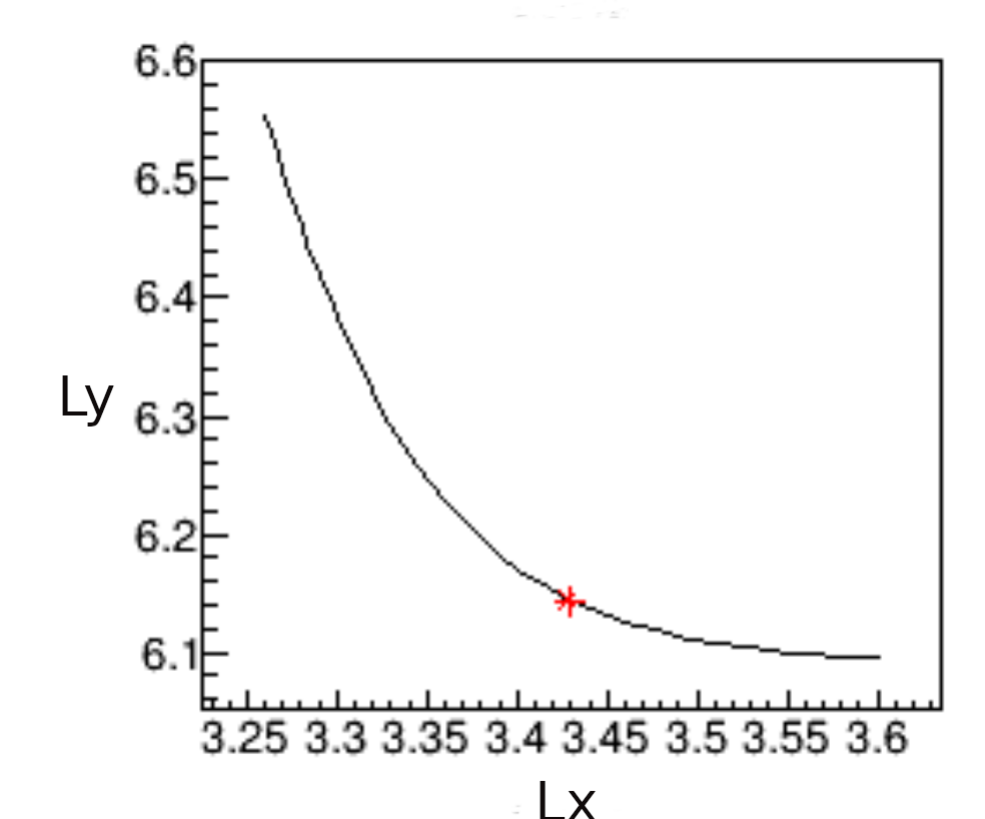
To avoid fluctuations on linear inversion of the response matrix [3].

$$L(x, \lambda) = L_1 + L_2$$

$$L_1 = (y - Ax)^T V_{yy}^{-1} (y - Ax)$$

$$L_2 = \tau^2 (x - f_b x_0)^T (L^T L) (x - f_b x_0) \quad (2)$$

L_1 is from a least square minimization and L_2 describes the regularization



- The read marker denotes the point for the optimum regularization strength (τ).

- At lower zenith angle (0° to 17°), the data exhibits a closer alignment with FLUKA-simulated models.
- At moderate zenith angle, Ghiesha shows better comparison.
- For large zenith angle data shows much lower ratio than all predictions.